JOURNAL OF SPACECRAFT AND ROCKETS
Vol. 42, No. 4, July–August 2005

Construction of a Unified Continuum/Kinetic Solver for Aerodynamic Problems

V. I. Kolobov,* S. A. Bayyuk,† and R. R. Arslanbekov‡
CFD Research Corporation, Huntsville, Alabama 35805
and
V. V. Aristov,§ A. A. Frolova,¶ and S. A. Zabelok**
Dorodnicyn Computing Center of the Russian Academy of Science, 119991, Moscow, Russia

We describe our progress toward the development of a unified flow solver (UFS) that can automatically separate nonequilibrium and near-equilibrium domains and switch between continuum and kinetic solvers to combine the efficiency of continuum models with the accuracy of kinetic models. Direct numerical solution of the Boltzmann transport equation is used in kinetic regions, whereas kinetic schemes of gas dynamics are used elsewhere. The efficiency and numerical stability of the UFS is attained by using similar computational techniques for the kinetic and continuum solvers and by employing intelligent domain decomposition algorithms. Different criteria for identifying kinetic and continuum areas and two different mechanisms of coupling Boltzmann and Euler solvers are explored. Solutions of test problems with small Knudsen number are presented to illustrate the capabilities of the UFS for different conditions. It is shown that the UFS can automatically introduce and remove kinetic patches to maximize the accuracy and efficiency of simulations. To our knowledge, this is the first attempt to use direct Boltzmann and continuum flow solvers for developing a hybrid code with solution adaptive domain decomposition.

I. Introduction

A VARIETY of flow problems are characterized by large variations of gas density and other macroscopic characteristics of the flow. Examples of such problems include gas distribution in the gravitational field of a planet, gas flows in nozzles, a gas rotating at high speed in a spinning cylinder. Another class of flow problems is characterized by the presence of nonequilibrium patches embedded in near-equilibrium flow regions. In these patches, which are associated, for example, with shock waves, contact discontinuities, shear or boundary layers, the state of the flow changes drastically over a relatively small distance. For aerospace applications, a spacecraft encounters different flow regimes while ascending to orbit or descending through an atmosphere to a planet's surface. On Earth, at altitudes of 90 km and above, the Knudsen number is large, corresponding to a rarefied-gas regime. At altitudes below 70 km, the Knudsen number is smaller, and the flow is well approximated by the continuum model using either the Euler or Navier–Stokes equations. For intermediate altitudes, in the transitional regime, the continuum flow equations cease to be valid in the boundary layers, but remain adequate in the far-field flow. The need for a hybrid solver arises from the fact that continuum models do not resolve kinetic effects, whereas global solutions with atomic scale resolutions are not feasible. Hybrid schemes that combine the efficiency of Navier–Stokes or Euler solvers in the continuum region with the accuracy of kinetic solvers in nonequilibrium areas have received increased attention since the early 1990s for both aerospace and microflow applications.[1]

Received 28 April 2004; revision received 22 September 2004; accepted for publication 1 October 2004.

*Manager, Plasma Technologies Branch. Member AIAA.
†Principal Research Engineer, Aeromechanics Branch.
‡Senior Research Scientist, Plasma Technologies Branch.
§Professor and Head, Gas Kinetic Theory Subdivision.
¶Group Leader and Senior Research Scientist.
**Research Scientist.

Two main approaches have been used for the numerical solution of the Boltzmann equation: the direct numerical solution (DNS) method and the direct simulation Monte Carlo (DSMC) method. Historically, DNS is one of the first methods of solving the Boltzmann equation.[2] It usually consists of two steps: the evaluation of the collision integral and the numerical integration of the differential part of the Boltzmann equation. The major advantages of DNS are uniform accuracy of computing both the low- and high-density regions of the flow and effective parallelization of the computational code. The limitations of the method are mainly related to dependence of the computational cost on the dimensionality of the problem and the resulting high computational cost for modeling three-dimensional problems.[3] Attempts to develop efficient deterministic methods remain an active area of research.[4,5]

The DSMC method has become de facto the main computational tool for studies of complex, multidimensional rarefied flows.[6,7] This is primarily because of its relative simplicity, the possibility of using various models of gas particle interactions and chemical reactions without substantial complications in the computational algorithm, and the possibility of effective use of parallel computers. Compared to DNS approaches, the computational cost of DSMC methods is proportional to the number of simulated particles. The method becomes too expensive for near-continuum flows because it requires the resolution of collisional length and collisional timescale. This is the primary motivation for the use of the continuum approach in parts of the flow where it is applicable. Owing to its statistical nature, the DSMC method often yields low-accuracy and noisy results relative to the DNS method, and it is difficult to match DSMC solvers with continuum solvers. The DSMC method also becomes inefficient for the low-Mach, high-Knudsen-number flows important for microflow applications. The information preserving (IP)-DSMC procedure has been proposed to address the challenges of the low speed rarefied flows.[8]

Attempts to develop hybrid DSMC/continuum solvers have been undertaken in a number of works (see Refs. 9 and 10 for the latest reviews). We briefly mention here a hybrid scheme by Eggers and Beylich,[11,12] where in regions with strong deviations from the equilibrium state the DSMC method was used, and in other regions a continuum scheme was used. In Ref. 13, a coupled Navier–Stokes–Boltzmann strategy has been introduced that uses locally a kinetic model in the boundary layer coupled through wall friction forces

to a global Navier–Stokes solver. Another approach was proposed by Bourgat et al.,[14] in which the coupling has been achieved for monoatomic and diatomic gases, and an adaptive coupling algorithm was developed that takes into account both the automatic decomposition of computational domains and the time-marching algorithm to couple the models. A property extrapolation technique was used by Wadsworth and Erwin[15] for the coupling the Navier–Stokes and DSMC solvers. Hash and Hassan[16] suggested that the Marshak condition is a better coupling technique. They also showed a significant impact of the large statistical scatter from the DSMC method. Recently, an adaptive mesh and algorithm refinement (AMAR) procedure, which embeds a DSMC-based particle method within a continuum grid, has been developed, enabling molecular based treatment within a continuum region.[17] In the AMAR procedure, the grid refinement is supplemented by algorithm refinement (continuum to atomistic) based on continuum breakdown criteria. Hybrid methods could provide significant savings by limiting molecular scale solutions only to the regions where they are needed.

A major challenge in the development of hybrid codes is the simultaneous use of kinetic and hydrodynamic models in a single code. The two major issues are the choice of a coupling method and the imposition of boundary conditions for the molecular simulations at interfaces. The different methods of coupling kinetic and continuum models that have been developed or proposed to date can be classified into three categories:

1) Domain decomposition in physical space is the first category. In this category, the computational domain is decomposed into kinetic and continuum subdomains using certain criteria.[17,18]

2) Domain decomposition in velocity space is next. In this category, one performs decomposition in velocity space to describe differently fast particles and slow particles.[19]

3) Hybrid models is the last category. In this category, one solves both the kinetic and the continuum equations in the entire domain and uses the distribution function to compute the transport coefficients for the fluid equations.[20,21]

This paper describes our progress toward the development of a unified flow solver (UFS) using solution adaptive domain decomposition in physical space. The feasibility of such an approach has been demonstrated in several papers.[22–24] Using the DSMC technique for simulations of the kinetic domain. The uniqueness of our approach consists in using the DNS for simulations of the kinetic domain. To our knowledge, this is the first attempt to use direct Boltzmann and continuum flow solvers for developing a hybrid code with solution adaptive domain decomposition. The recent efforts described in Ref. 25 are similar but use a priory decomposition of the domain, not a dynamic automatic decomposition as in this work.

Using DNS instead of DSMC offers several advantages for building a unified flow solver. One of the major problems with coupling a DSMC and a Navier–Stokes (NS) code is related to the statistical nature of the DSMC. Because of strong fluctuations of the moments calculated from the DSMC distribution functions, the problem of connecting two regions is complicated by rather severe stability problems when DSMC data are handed over to continuum solver at the interface.[26] These fluctuations result in irregular boundaries. Using DNS allows much more manageable coupling of the continuum and kinetic domains.

In this paper we consider two different numerical schemes for the UFS for a simple one-component gas. Section II describes two DNS methods for the Boltzmann equation and presents examples of rarefied flow simulations using these solvers. Section III describes kinetic schemes for the continuum equations. Section IV is devoted to identification of kinetic domains and continuum breakdown criteria. Section V describes two strategies for the construction of the UFS and presents examples of hybrid solutions.

II. Numerical Solutions of the Boltzmann Equation

The main equation of rarefied gas dynamics is the Boltzmann transport equation (BTE), which describes the evolution of a one-particle distribution function in a six-dimensional phase space[27]

$$\frac{\partial f}{\partial t} + \boldsymbol{\xi}\cdot\nabla f = N - \nu f \tag{1}$$

The right-hand side of Eq. (1) contains operators that describe binary collisions among particles:

$$\nu = \int_R\int_S \sigma(|\boldsymbol{\xi}-\boldsymbol{\xi}_1|,\omega)|\boldsymbol{\xi}-\boldsymbol{\xi}_1| f(\boldsymbol{\xi}_*)\,\mathrm{d}\omega\,\mathrm{d}\boldsymbol{\xi}_*$$

$$N(f,f) = \int_R\int_S \sigma(|\boldsymbol{\xi}-\boldsymbol{\xi}_1|,\omega)|\boldsymbol{\xi}-\boldsymbol{\xi}_1| f(\boldsymbol{\xi}') f(\boldsymbol{\xi}'_*)\,\mathrm{d}\omega\,\mathrm{d}\boldsymbol{\xi}_*$$

where ω is a unit vector on a unit sphere S in velocity space; $\mathrm{d}\omega$ is an element of the area of the surface of this sphere, where ($\boldsymbol{\xi}'$, $\boldsymbol{\xi}'_*$) represent the postcollisional velocities associated with the precollisional velocities ($\boldsymbol{\xi}$, $\boldsymbol{\xi}_*$) and the collisional parameter ω; and the kernel σ describes the details of the binary interactions. In the present paper we only consider the traditional rigid-sphere model of intermolecular collisions. We will briefly describe our numerical schemes for solving the Boltzmann equation. Standard dimensionless notations[28] are used.

A. Conservative Splitting Method

The first scheme is the conservative splitting method (CSM).[29] This method splits the solution into two stages: collisionless flow and relaxation. For the collisionless flow stage we apply the following scheme for different signs of velocity components:

$$\frac{f^{*k}_{i\beta} - f^{k-1}_{i\beta}}{\Delta t} + \xi_\beta \frac{f^{k-1}_{i+1/2,\beta} - f^{k-1}_{i-1/2,\beta}}{\Delta x} = 0 \tag{2}$$

here * denotes the intermediate level, $f^{k-1}_{i+1/2,\beta} = (f^{k-1}_i + f^{k-1}_{i+1})/2 - \mathrm{sign}(\xi_\beta)(f^{k-1}_{i+1} - f^{k-1}_i)/2$, $i = (i_X, i_Y, i_Z)$ is the three-dimensional spatial index, Δx is the three-dimensional spatial step $(\Delta x, \Delta y, \Delta z)$, and $\beta = (\beta_X, \beta_Y, \beta_Z)$ is the velocity index.

The homogeneous relaxation stage has the form

$$\frac{f^{**k}_{i\beta} - f^{*k}_{i\beta}}{\Delta t} = \frac{1}{Kn}\left(-\nu^{*k}_{i\beta} f^{**k}_{i\beta} + N^{*k}_{i\beta}\right) \tag{3}$$

This implicit (explicit-implicit) scheme is absolutely stable, which is important if we wish to study physical instabilities with this method. For the conservative splitting method, a Monte Carlo evaluation of the collision integrals was used in this work. For the conservative splitting method, the so-called hydrodynamic conservation is maintained by using a correction procedure.

B. Discrete Velocity Conservative Method

Another method is the discrete velocity conservative method, which has been presented in detail in Ref. 30 and used in Ref. 31. In this method, kinetic conservation is maintained by satisfying the conservative laws for the full collision integral. For evaluation of the collision integral, both the quasi Monte Carlo method with Korobov sequences and the deterministic "node-to-node" (NtN) method in velocity space have been used. The scheme without splitting for this method is written as follows:

$$\frac{f^k_{i\beta} - f^{k-1}_{i\beta}}{\Delta t} + \xi_\beta \frac{f^{k-1}_{i+1/2,\beta} - f^{k-1}_{i-1/2,\beta}}{\Delta x} = \frac{1}{Kn}\left(-\nu^{k-1}_{i\beta} f^{k-1}_{i\beta} + N^{k-1}_{i\beta}\right)$$

The main characteristic of the NtN method is the possibility to use all nodes of a selected computational domain in velocity space and to develop a completely implicit scheme for steady-state problems or to use an implicit-explicit scheme where the collision frequency $\nu(\xi)$ and the integral of inverse collisions are taken from the preceding time step. When calculations of the collision integrals employ a Monte Carlo or a quasi Monte Carlo procedure for selecting velocity nodes of colliding molecules, then it is possible to use a partially implicit scheme in the form

$$\frac{f^k_{i\beta} - f^{k-1}_{i\beta}}{\Delta t} + \xi_\beta \frac{f^{k-1}_{i+1/2,\beta} - f^{k-1}_{i-1/2,\beta}}{\Delta x} + \frac{\nu^{k-1}_{\max}}{Kn} f^k_{i\beta}$$

$$= \frac{1}{Kn}\left(\nu^{k-1}_{\max} - \nu^{k-1}_{i\beta}\right) f^{k-1}_{i\beta} + N^{k-1}_{i\beta}$$

where $\nu_{\max} = \max_\xi \nu(\xi)$ and $f^k_{i+1/2,\beta}$ is the flux, calculated using first- or second-order accurate approximation. Such an iterative procedure allows us to increase the time step and is very useful for steady-state problems with small Knudsen number.

C. Coordinate System

For the test cases shown next, cylindrical coordinate systems were used with radius and angle r, ϕ. The Boltzmann equation (1) in this coordinate system has the form

$$\frac{\partial F}{\partial t} + \frac{\partial \Phi}{\partial r} + \frac{\partial \Psi}{\partial \varphi} = \frac{1}{JKn} I(f, f) \tag{4}$$

where $F = f/J$, $\Phi = fU/J$, $\Psi = fV/J$, and J is the Jacobian of the transformation. The quantities U and V denote the contravariant components of the velocity vector.

To correctly account for the behavior of the distribution function near the body, the grid is stretched toward the surface according to the equation

$$r_i = -Kn/\alpha \, \ell_n[1 - (1 - Kn)i/N_2], \qquad i = 0, 1, \ldots . N_1, N_1 \le N_2$$

where α, N_1, N_2 are parameters, defining the value of the steps and the number of points in the Knudsen layer. Equation (4) on the grid r_{ij}, φ_{ij} is

$$\frac{F^{k+1}_{ij} - F^k_{ij}}{\tau_{ij}} + \frac{\Phi^k_{i+\frac{1}{2},j} - \Phi^k_{i-\frac{1}{2},j}}{h_r} + \frac{\Psi^k_{i,j+\frac{1}{2}} - \Psi^k_{i,j-\frac{1}{2}}}{h_\varphi}$$

$$= \frac{1}{JKn} I\left(f^k_{ij}, f^k_{ij}\right) \tag{5}$$

where

$$\Phi_{i+\frac{1}{2},j} = F_{i+\frac{1}{2},j} U_{i+\frac{1}{2},j}, \qquad \Psi_{i,j+\frac{1}{2}} = F_{i,j+\frac{1}{2}} V_{i,j+\frac{1}{2}}$$

Here the fluxes, $F_{i+\frac{1}{2},j}$, $F_{i,j+\frac{1}{2}}$ are given by

$$F_{i+\frac{1}{2},j} = G\left(F_{i,j} + \delta^x F_{i,j}, F_{i+1,j} + \delta^x F_{i+1,j}, U_{i+\frac{1}{2},j}\right)$$

$$F_{i,j+\frac{1}{2}} = G\left(F_{i,j} + \delta^y F_{i,j}, F_{i,j+1} + \delta^y F_{i,j+1}, V_{i,j+\frac{1}{2}}\right)$$

and the function G is given by

$$G(a, b, c) = (a + b/2) - \text{sign}(c)[(b - a)/2]$$

The additional flux limiting terms $\delta^x F$, $\delta^y F$ are evaluated from the relations

$$\delta^x F_{i,j} = \tfrac{1}{2}\text{mid}(F_{i+1,j} - F_{i,j}, F_{i,j} - F_{i-1,j})$$

$$\delta^y F_{i,j} = \tfrac{1}{2}\text{mid}(F_{i,j+1} - F_{i,j}, F_{i,j} - F_{i,j-1})$$

where function $\text{mid}(a, b)$ is chosen from one of the following two forms:

$$\text{mid}(a, b) = \begin{cases} \min(|a|, |b|)\text{sign}(a), & ab > 0 \\ 0, & ab \le 0 \end{cases}$$

or

$$\text{mid}(a, b) = \frac{(|ab| + ab)\text{sign}(a)}{|a + b|}$$

To obtain the second-order approximation in time, the following predictor–corrector procedure is used:

$$\bar{F}^{k+1}_{ij} = F^k_{ij} - \tau_{ij} A(F^k)$$

$$F^{k+1}_{ij} = \tfrac{1}{2}\left[F^k_{ij} + \bar{F}^{k+1}_{ij} - \tau_{ij} A(\bar{F}^{k+1})\right]$$

where

$$A(F^k) = \left[\frac{\Phi^k_{i+\frac{1}{2},j} - \Phi^k_{i-\frac{1}{2},j}}{h_r} + \frac{\Psi^k_{i,j+\frac{1}{2}} - \Psi^k_{i,j-\frac{1}{2}}}{h_\varphi} - \frac{1}{JKn} I(f^k, f^k)\right]$$

D. Examples of Calculations

We illustrate the application of the two DNS schemes just described to simulation of external flow around a cylinder. We consider a problem in which the Mach number is 3 and the temperature of the wall T_r is equal to 4. First, we solve the Boltzmann equation using the CSM with a Monte Carlo evaluation of the collision integrals. The velocity space was discretized using a uniform grid with (22, 22, 11) nodes. For Monte Carlo evaluation of the collision integrals, 100 random trials were used. A spatially nonuniform grid along the radial direction, with exponential dependence of the step size on the distance from the surface of the cylinder, was used to resolve the details of the boundary layer. In Fig. 1, the density contours are shown for a case with $Kn = 0.1$, using a grid with 100 nodes along the radius and 60 nodes in the circumferential direction. One can see the formation of the bow shock wave. Comparison of this result with the corresponding density contour plot obtained using the NtN scheme shows good agreement.

Figure 2 shows the simulation results for this problem with $Kn = 0.01$, obtained by the CSM using spatial grid with 150 nodes along the radius and 75 nodes in the circumferential direction. The computational domain was bounded by a circle with radius $R = 10$. One can see that the shock wave for $Kn = 0.01$ has a higher gradient across it (in comparison with the case for $Kn = 0.1$), and its position is closer to the cylinder.

For the NtN method, the computational domain was bounded by the circle with radius $R = 4$, and the grid had (100,90) nodes in physical space and (24, 24, 12) nodes in velocity space. The Mach-number contours obtained by the NtN method are presented in Fig. 3. The location of the sonic line (part ab) is close to that obtained for the same problem using the Euler equations. The part of the line bc is determined by the solution in the Knudsen layer and is connected with the boundary condition at the wall of the cylinder. Note that

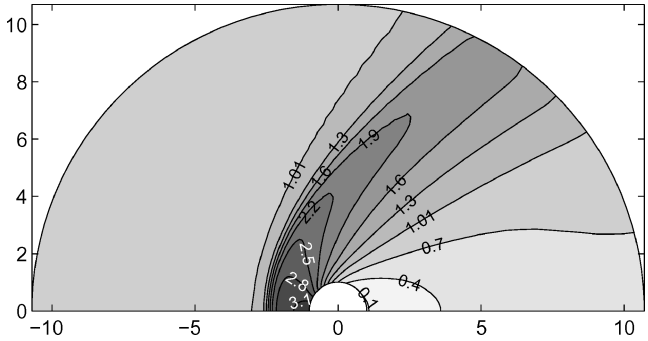

Fig. 1 Density contours obtained with the CSM for a Mach 3 flow over a cylinder, with $Kn = 0.1$.

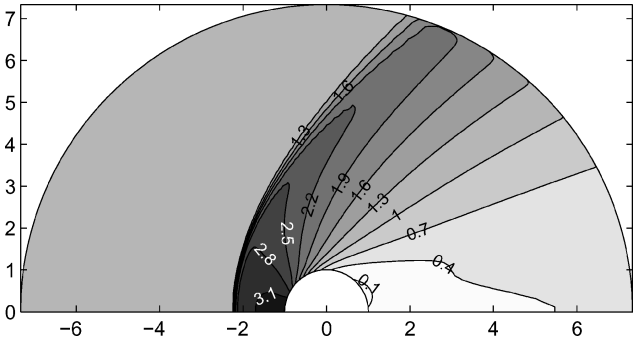

Fig. 2 Density contours obtained with the CSM for a Mach 3 flow over a cylinder, with $Kn = 0.01$.

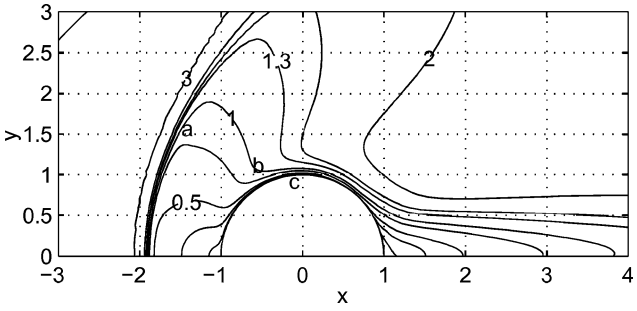

Fig. 3 Contours of the Mach number for a Mach 3 flow around a cylinder.

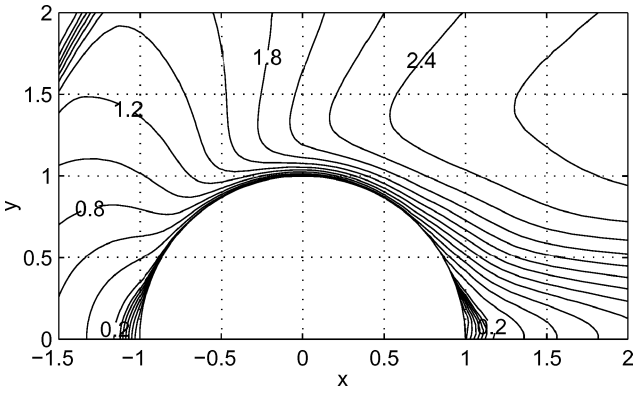

Fig. 4 Mean velocity contours near the surface of cylinder in a Mach 3 flow.

accurate prediction of the spatial location of the sonic line is one of the important criteria for such computations. In addition to the location of the sonic line, an important measure of the accuracy of a gasdynamic computation is the correct location of discontinuities. The location of the shock is consistently predicted by all schemes, even when using different grids. This is typically true for schemes that satisfy the conservation property.

Figure 4 shows the velocity contours near the surface of the cylinder. Detailed solution in the Knudsen layer (which in this case has dimensions of order 0.01, for $Kn = 0.01$) is possible with our method.

It is important to compare the solutions obtained by the two DNS methods to ensure the reliability of the Boltzmann solver. For both methods, a mesh-refinement study was carried out, but only with the spatial mesh because the velocity mesh was deemed to be sufficiently fine. Comparison for $Kn = 0.1$ is satisfactory in all points of the computational domain. Comparison for $Kn = 0.01$ is satisfactory at least near the surface of the cylinder, which is the most interesting region for this investigation. In Fig. 5, comparison of the density distributions around the body demonstrates good agreement for the results of the two methods. A quantitative comparison is presented in Fig. 6, where the density distribution is shown along the symmetry axis for coordinates between -1.5 and -1 (in front of the body) and between 1 and 2 (behind the body). The density distribution at the surface of the body is given as the projection to the symmetry line with coordinates between -1 and 1.

III. Kinetic Schemes for the Continuum Equations

Traditional numerical schemes for computational fluid dynamics (CFD) are based on discretization of the continuum (Euler or Navier–Stokes) equations. The continuum equations can be derived from the BTE, and the macroscopic gas dynamic parameters (such as the density, velocity, and temperature) are calculated as moments of the particle distribution function (PDF). Kinetic schemes for continuum equations differ from the traditional CFD schemes by using the BTE for building the corresponding computational CFD algorithms.

Kinetic schemes for the Euler equations (using the equilibrium distribution function) have been proposed in Refs. 32 and 33 and independently in Refs. 34 and 35. Note also that the main idea of this

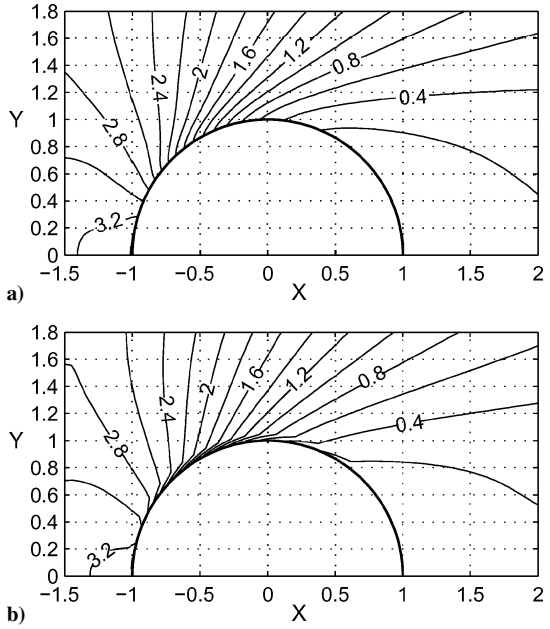

Fig. 5 Comparison of the contours of the density distributions about the body by two direct methods: a) the CSM and b) the NtN.

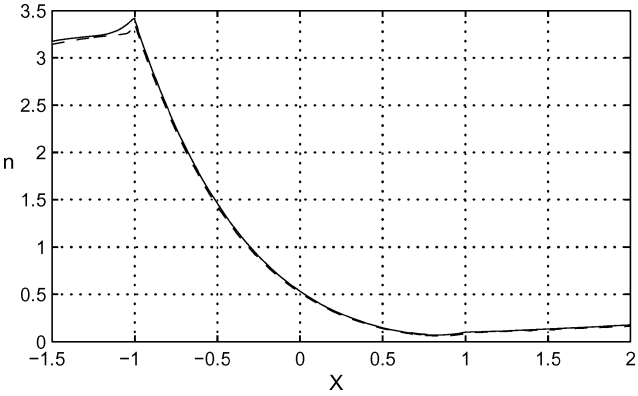

Fig. 6 Comparison of density distributions in the symmetry line and in the surface of the body by two direct methods: ——, CSM and – – –, NtN.

approach has been suggested earlier, in Ref. 36. Kinetic schemes using moments of the equilibrium distribution function have been used by Deshpande with coauthors[37] and have been further developed and improved (see Refs. 38–41). Kinetic schemes are preferable for developing hybrid codes because the BTE is used as foundation for both algorithms.

We have developed a kinetic scheme for the Euler equations that consists of collisionless flow followed by Maxwellization. In this scheme, the stage of collisionless flow is the same as for the Boltzmann solver, while the uniform relaxation stage is replaced by the Maxwellization of the distribution function. The third stage is the conservative correction that ensures the positivity of the distribution function. The use of correction is significant for the asymptotic kinetic Euler scheme because the errors of these schemes are larger than those for the Boltzmann scheme: in the latter case, the errors are proportional to the value of the time step and to the value of the velocity step, and in the former case they are proportional only to the velocity step. We used the correction in which the density, mean velocity, and temperature are changed in such a way that the first five moments from the corrected function are equal to the values of these moments in the Euler scheme. Newton iterations were used. For the Boltzmann solver, the ordinary form of correction[3] has been used.

An example of two-dimensional simulations using the kinetic scheme for the Euler equations for the problem of a Mach 3 flow around a cylinder described earlier demonstrates a qualitatively correct picture of the shock-wave structure (see Fig. 7). We emphasize

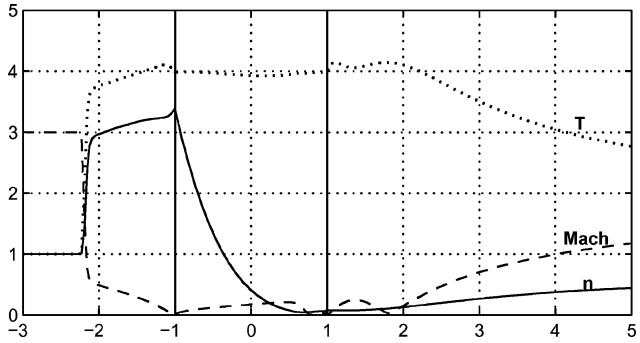

Fig. 7 Density, temperature, and Mach-number distributions along the symmetry line and on the surface of the body obtained by the kinetic Euler solver.

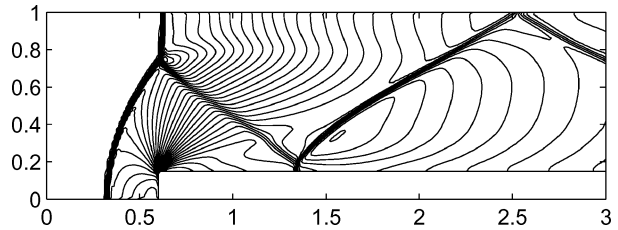

Fig. 8 Density contours: $t = 4$ and $N = 240 \times 80$.

that the same kinetic boundary condition (diffuse reflection) was used at the body surface as in the case of the Boltzmann equation. This model combines the kinetic and continuum properties. For adequate comparison with the traditional gasdynamics solution, one should use specular reflection at the solid boundary.

Another approach to the kinetic Euler scheme is based on the Euler flux method.[42] The main idea of this method consists of the calculation of fluxes on cell faces as a sum of half-fluxes. These half-fluxes are calculated analytically based on the Maxwellian distribution. We have used the variant of this method based on the work of Ref. 43.

The analytical values of the half-fluxes are given by

$$\Psi^{\pm}_{i+\frac{1}{2}} = \int_{\xi \gtrless 0} \xi \psi f^{M}_{i+\frac{1}{2}} \, \mathrm{d}\xi$$

where ψ denotes collision invariants

$$\psi = \left[1, \xi_x, \left(\xi_x^2 + \xi_y^2 + \xi_z^2\right)\right]$$

and $f^{M}_{i+1/2}$ denotes the Maxwellian distribution with local parameters ρ_i', u_i, T_i for $\xi_x > 0$ and the Maxwellian distribution with parameters ρ_{i+1}, u_{i+1}, T_{i+1} for $\xi_x < 0$. To obtain the second-order scheme, we used the flux limiter technique and the predictor–corrector procedure already described.

We illustrate our kinetic scheme for a two-dimensional simulation of internal gas flow in a channel with a forward-facing step. The channel has length equal to 3, height equal to 1, and a step height equal to 0.2. The step is located at 0.6 of the length unit from the entrance of the channel. This two-dimensional problem has been used routinely for checking accuracy of numerical schemes.[44] The accuracy of a scheme can be checked by the correctness of the time-dependent structure of the shock-wave pattern and associated property jump at $t = 4$. The model gas in Ref. 44 has a ratio of specific heats $\gamma = 1.4$. At $t = 4$, position of the triple point is precisely above the corner of the step. The flow configuration is characterized by the presence of a contact discontinuity and three reflected shock waves. Because in our simulations $\gamma = 5/3$ was used, to obtain the same time evolution of the flow, we must change the height of the step to 0.15. At the walls of the channel and at the step surface, reflecting boundary conditions are applied. Calculations are carried out with second-order accuracy in space and time. Results of the calculation at $t = 4.0$ are presented in Fig. 8. It is seen that the bow shock wave and the oblique weak shock waves are well resolved, but the contact discontinuity is rather smeared. The position of the Mach stem is correctly predicted. The smearing of the contact discontinuity is not only a consequence of the scheme's viscosity, but also result of the kinetic boundary conditions at the walls.

IV. Coupling Kinetic and Continuum Models: Criteria for Switching

The construction of a unified rarefied/continuum solver involves the specification of local rarefaction criteria. This important problem is widely discussed in the literature. In our point of view, the criteria for switching numerical schemes from the continuum to the kinetic must be simple and natural because both schemes (the kinetic Boltzmann and the kinetic continuum) possess common features. In developing these criteria, we have to take into account the experience of previous works on construction of hybrid schemes involving the BTE and NS equations. But first we begin our study from an analysis of simple criteria for switching algorithms from Boltzmann to continuum kinetic algorithms. We can distinguish between the two types of such criteria, which can be labeled "kinetic criteria" and "gradient criteria." The former are connected with the computation of the collision integrals of the BTE or its high-order moments (such as the components of the stress tensor), which tend to zero in equilibrium. The latter are connected with the computation of spatial gradients of quantities of the order of unity (such as the density, the mean velocity, and the temperature), which determine the local Knudsen number. Each of these criteria has advantages and disadvantages.

An attractive kinetic criterion was proposed by Tiwari.[24] In that paper, the "grad" expression for the distribution function was analyzed, and a parameter based on a combination of the stress tensor components and the heat flux was introduced. If this parameter was smaller than a breakdown value (which in Tiwari's paper was set equal to 0.4), the continuum model (that is, the Euler equations) was used; otherwise, the kinetic model (which was a DSMC scheme) was used.

Another kinetic (or "collisionality") criterion was proposed by A. Frolova and expressed in the form

$$S = \log\left(\frac{\int |-\nu f + N| \, \mathrm{d}\xi}{\int \nu f \, \mathrm{d}\xi}\right) \tag{6}$$

using the notations of Eq. (1). The value of S specifies the deviation from the Maxwellian of the local PDF and hence can be taken as a measure of the error obtained by replacing the Boltzmann equation by the Euler equations or by a kinetic equation with instant Maxwellization. Large negative values of S correspond to small values of the full collision integral. In Fig. 9, the value of S is presented for $t = 10$ when the solution has reached a steady state. Dark areas correspond to large negative values of S. From comparison of the density contours in Fig. 2 with the S contours in Fig. 9, one can judge in which parts of the computational domain the fluid equations (Euler or Navier–Stokes) should be used, and in which parts the Boltzmann equation should be used.

The use of the kinetic criterion (6) is not simple because one must compute complex collision integrals at each spatial point. Note,

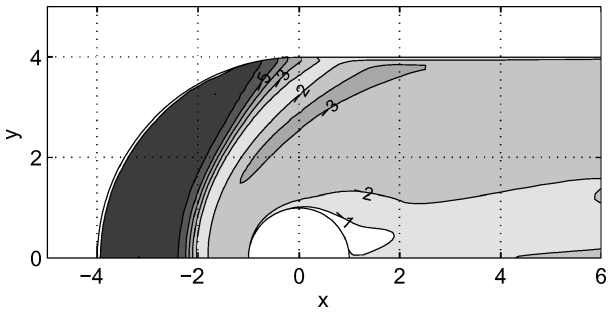

Fig. 9 Quantity S at $t = 10$.

however, that this difficulty applies in general to all kinetic criteria derived from the kinetic solver, including Tiwari's criterion too. Computation of a small value with a high accuracy as required in this case typically causes many difficulties. In a general case, the magnitude of the error in the computation can be larger than the values of the heat flux, or the stress tensor components, and the full collision integral that vanishes when the Knudsen number tends to zero.

The gradient criteria relate to the local Knudsen number. A typical choice for such a criterion is the density gradient or gradients of other macroparameters. Parameters defined by means of the local spatial characteristics have advantages compared to kinetic characteristics because one does not require a high accuracy in computing small values of the order of the Knudsen number. The simplest characteristic has the following form:

$$Kn_L = \lambda|\nabla n|/n \tag{7}$$

where Kn_L is a local Knudsen number and λ is the mean free path. A continuum breakdown criterion of this type was considered by Bird.[45] More general expressions with multiple flow properties (which are computed as gradients) have been applied in Refs. 46 and 47. The latter criteria differ from the Bird criterion where the length scale is based on a projection of the density gradient along a streamline. We used the density gradient criterion in simulations described next. Figure 10 shows spatial distributions of the continuum and kinetic domains obtained with the gradient criterion (7) for the case presented in Fig. 8.

A general breakdown criterion using the gradients of the mean velocity u and the temperature T, which are indicators of the breakdown of the Navier–Stokes equations in the presence of thermal nonequilibrium, can be defined as follows:

$$Kn_L = \lambda[(\nabla n/n)^2 + \nabla u^2/u^2 + (\nabla T/T)^2]^{\frac{1}{2}}$$

Using gradient criteria is natural in hybrid methods based on the flux-kinetic approach for continuum equations (of Xu's type[39]), because these types of kinetic-continuum methods deal with the moments, not with the distribution function. However, the hybrid methods dealing with distribution function can also benefit from the gradient criteria determined locally in every cell. The gradient criteria have been used in this work with the conservative splitting method, in addition to the evaluation of the collision integrals.

Figure 11 shows the distribution of the continuum breakdown parameter based on the kinetic criteria derived from components of the stress tensor, $\delta_2 = [(p_{xx})^2 + (p_{yy})^2]^{1/2}$.This breakdown parameter is simpler and more economical to compute because it does not require evaluation of the collision integrals as in kinetic criterion (6).

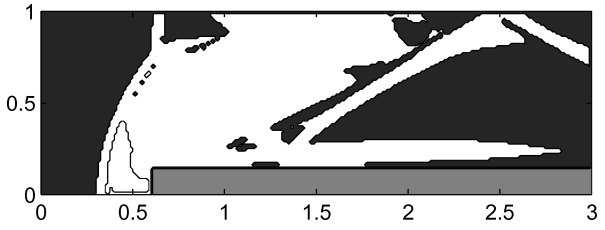

Fig. 10 Distribution of continuum (black) and kinetic domains.

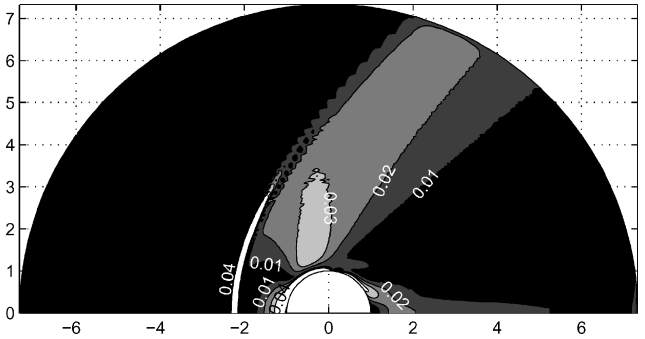

Fig. 11 Distribution of the breakdown parameter δ_2 for $Kn = 0.01$.

V. Unified Method with Automatic Domain Decomposition

We have explored two main strategies for constructing hybrid codes. The first one is a combination of the node-to-node direct Boltzmann solver with the kinetic continuum method using moments of the equilibrium distribution function (see Refs. 29, 33, and 32). The second one is the conservative splitting Boltzmann solver (with Monte Carlo or deterministic methods for evaluation of the collision integrals) and kinetic continuum scheme using the equilibrium distribution function.

A. Unified Solver with Kinetic Scheme Using Moments (Half-Fluxes)

The main problem in creating gas-kinetic schemes is obtaining the correct fluxes at cell interfaces. Having an analytical solution of the problem on the basis of the Boltzmann equation, we should be able to construct the numerical scheme as an extension of the Godunov method. Without an analytical solution, we calculate the fluxes at the cell interfaces based on a difference scheme of the Boltzmann solver, assuming the distribution function is equal to a Maxwellian and that the collision integral is equal to zero.

For simplicity we describe the construction of the hybrid method for a one-dimensional case. The deterministic conservative method of discrete coordinates is used to solve the Boltzmann equation in the nonequilibrium regions. The finite difference scheme for the convective part of the Boltzmann equation has the same form as Eq. (2). Collision integrals are calculated with the deterministic node-to-node method.

For constructing a hybrid method, the computational domain can be decomposed into the equilibrium region and the kinetic one with the help of the mentioned breakdown parameter $\beta = Kn_L$ computed in terms of the gas density gradient.

Note that we use here the kinetic/continuum method, which uses only moments of the equilibrium distribution function. The NtN scheme does not use splitting. Therefore, it is not a simple problem to obtain for this approach the distribution function for the continuum scheme. The kinetic-moments approach leads naturally to the gradients criteria where these moments appear.

Let us choose two values (a, b) for the breakdown parameter β. At each time step we define the sets of nodes

$$M_a = \{i \mid \beta < a\}, \qquad M_b = \{i \mid \beta > b\}, \qquad M_{ab} = \{i \mid a \le \beta \le b\}$$

The fluxes $\Psi_{i+1/2}$ are calculated either through numerical quadrature formulas or by using analytical values (3). If the node $i \in M_{ab}$, the flux $\Psi_{i+1/2}$ is calculated with both procedures. The resulting fluxes are constructed by means of the interpolation formula

$$\Psi_{i+\frac{1}{2}} = h(\beta)\Psi^a_{i+\frac{1}{2}} + [1 - h(\beta)]\Psi^b_{i+\frac{1}{2}}$$

with $h(\beta = (\beta - a)/(b - a)$. Thus, the flux at a node $i \in M_{ab}$ is obtained by averaging of the kinetic and equilibrium values.

Figure 12 shows the pressure evolution for a one-dimensional Riemann problem calculated by the hybrid method. The initial values of the parameters are (on the left and right, respectively) $P_l = 12$, $T_l = 4$, $\rho_l = 3$, $u_l = 0.3$, $P_r = 1$, $T_r = 1$, $\rho_r = 1$, and $u_r = 0$. The parameters for the code switching are $a = 0.02$, $b = 0.02$. A solution to this problem with the Euler equations represents a rarefaction wave (moving to the left of the discontinuity), a shock wave (moving to the right of the discontinuity), and a zone of uniform pressure between them.

B. Unified Solver with Kinetic Scheme by Using Distribution Function

Our second strategy toward hybrid rarefied/continuum solver is based on the approach described in Refs. 22 and 23. In these works, the Euler equations are solved by splitting the evolution into a advection step and a Maxwellization. Although in this approach the

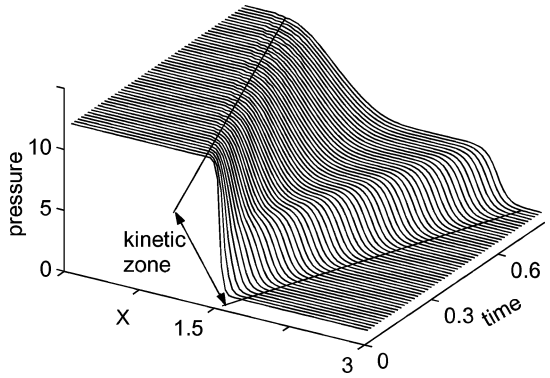

Fig. 12 Pressure distribution for the Riemann problem obtained by hybrid method.

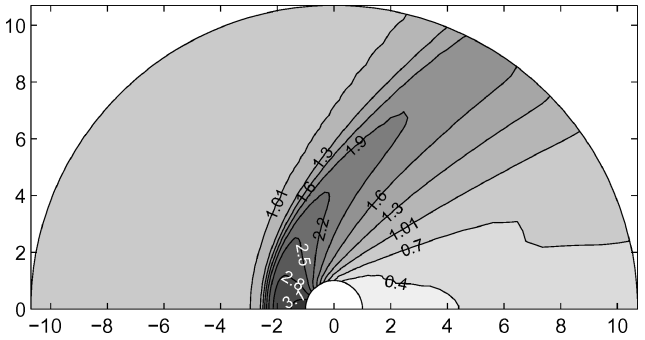

Fig. 13 Density contours obtained with the hybrid solver for $M = 3$, $Kn = 0.1$.

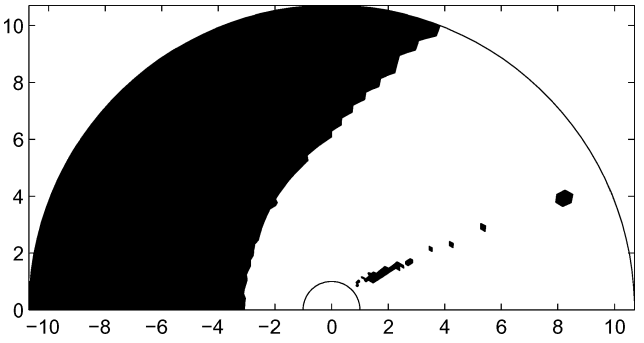

Fig. 14 Distribution of continuum (black) and kinetic domains for $M = 3$, $Kn = 0.1$.

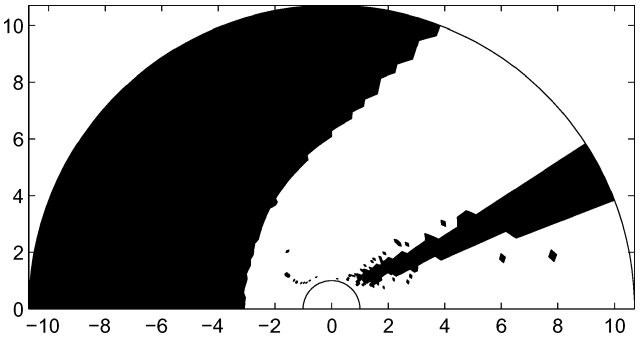

Fig. 15 Domain decomposition via a hybrid method. The white regions correspond to Boltzmann kinetic solver, and the black regions correspond to the continuum Euler solver.

distribution function is used, the computation of collision integrals with Maxwellian distribution is less expensive than the computation of generic collision integrals. Hence, the hybrid method could still be significantly less expensive than the pure Boltzmann method.

We use a simple kinetic criterion to determine the breakdown parameter. The calculation of stress and heat flux can be made at every point of the computational domain where the distribution function is known. These quantities could be useful for evaluation of numerical errors and for defining a background value of the kinetic breakdown parameter. For this purpose, we can use one of the stress tensor components. Let us assume that this quantity is computed for the equilibrium function with an error of ε. Then this value of ε defines the background level of the breakdown parameter. Outside nonequilibrium zones for small Knudsen number, this quantity, according to Chapman–Enskog theory, is proportional to the rarefaction parameter. Let us assume $\varepsilon = 0.001$. With the accuracy of the factor, we can say that we might not resolve zones with a local Knudsen number equal to 0.001. But if this level of accuracy is sufficient for the purposes of our investigation, we can choose the value of ε as a magnitude of the breakdown parameter.

We have attempted to apply the kinetic criterion just mentioned for construction of a hybrid scheme for moderate Knudsen number, $Kn = 0.1$, where the continuum and rarefied (nonequilibrium) zones are distinctly seen. First, we used the modulus of one of the stress tensor component (for instance $|p_{xx}|$) as the breakdown parameter. In zones where $\delta_1 = |p_{xx}| \leq \varepsilon$, we used the kinetic gasdynamic approximation, whereas in zones where $\delta_1 = |p_{xx}| > \varepsilon$ we used the Boltzmann solver. The algorithm is very simple. The collisionless stage of splitting is common for all cells of the computational domain. The relaxation process for the continuum cells involves local Maxwellization of the distribution function, whereas in kinetic cells involve calculation of the Boltzmann collision integral. In this approach, there is no need to apply any interface boundary conditions between the continuum and kinetic cells. This approach is similar to some extent to Tiwari's hybrid method.

For our first hybrid calculation, we took $\varepsilon = 0.001$. This is the level of the error of the computation of the mentioned stress tensor component for the equilibrium distribution. In Fig. 13 we present the density contours. One can see that the density profile is similar to that shown in Fig. 1. Some nonsmooth regions are observed behind the cylinder, where the Euler equations are solved. It can be seen that near the body surface the contour density distribution is similar to that in Fig. 1.

In Fig. 14, the distribution of the continuum and kinetic areas in the computational domain is given. One can see that for this case, with a low level of the breakdown parameter, the continuum zones (black) appear only in front of the bow shock wave and in a few "spots" behind the cylinder.

The density profiles from the Boltzmann solver and those from the hybrid scheme on the axis of symmetry are so close that one cannot distinguish between the results obtained by the two solvers. The comparison of the density profiles along the symmetry axis behind the cylinder where the density is small shows that there is little difference in the spatial distributions obtained from the Boltzmann solver and those obtained by the hybrid scheme.

The next computation was performed for the same flow conditions using the breakdown parameter value of $\varepsilon = 0.002$. It can be seen in Fig. 15 that the continuum regions (black) are larger than those in Fig. 14. The CPU time for the kinetic-Euler scheme is more than one order of magnitude lower than it is for the pure Boltzmann scheme (for 100 random trials in the Monte Carlo evaluation of the collision integrals), resulting in a speed-up of the computations. When the black area is approximately equal to the white area, then the CPU time of the hybrid scheme is approximately half of the CPU for the pure BTE.

The first evidence of the influence of the breakdown parameter on the integral flow characteristics is given in Fig. 16, where the angular distribution of the density near the cylinder is presented. Here, the angle -90 deg corresponds to the symmetry line ahead of the cylinder, while the angle $+90$ deg corresponds to the symmetry line behind the cylinder. It is seen that a small difference between the curves is noticeable only behind the cylinder.

In the case $Kn = 0.01$, we used the other breakdown parameter, namely, $\delta_3 = [(p_{xx})^2 + (p_{yy})^2 + (p_{zz})^2]^{1/2}$. In regions where $\delta_3 \leq \varepsilon$, we used the kinetic gasdynamic approximation, whereas in regions where $\delta_3 > \varepsilon$ we used the Boltzmann solver. Figure 17 shows an

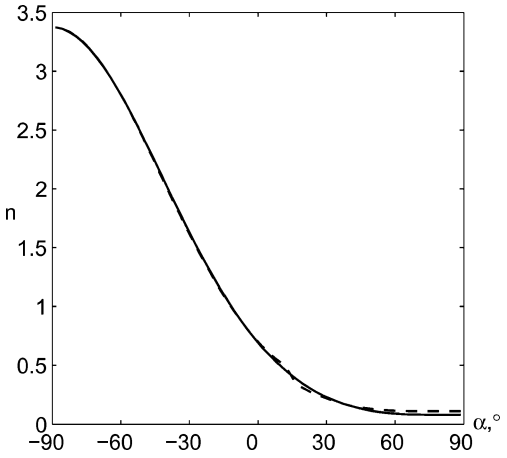

Fig. 16 Density dependence on the angle along the cylinder boundary: ——, Boltzmann solution and – – –, hybrid method.

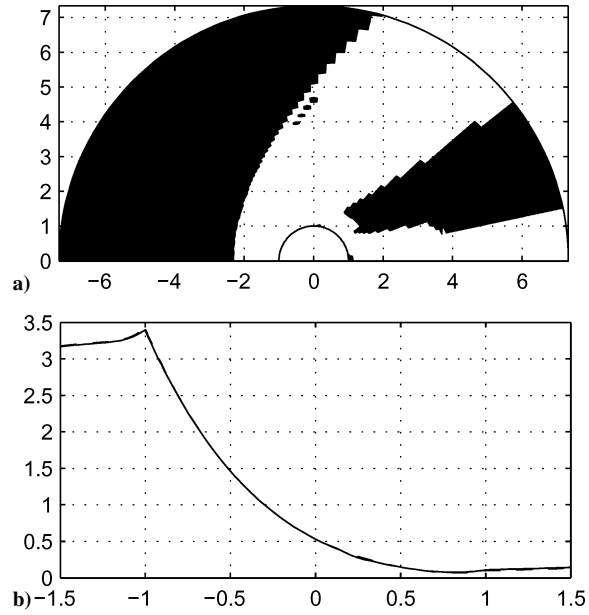

Fig. 17 Domain decomposition via a hybrid method (a). The white regions correspond to Boltzmann kinetic solver, and the black regions correspond to the kinetic Euler solver. b) The distributions of density along the symmetry line and on the surface of the cylinder: ——, hybrid method and – – –, Boltzmann solution.

example of hybrid simulations for a supersonic flow over a cylinder with $\varepsilon = 0.002$ for $M = 3$ and $Kn = 0.01$. Despite the sufficiently low level of the breakdown parameter for this case, the continuum zones (black) appear not only in front of the bow shock wave, but also behind the cylinder. The density at the surface of the cylinder from $x = -1$ to 1 as projected on the symmetry line is shown on the right-hand side of the figure.

The hybrid scheme just described is a simple continuum-kinetic model with one parameter ε being used to determine the extent of rarefaction of a flow (that is, the character of the spatial distribution of rarefaction of a flow is identified only by the magnitude of ε). If ε tends to zero, we obtain a pure Boltzmann model; if ε ends to infinity, we obtain a pure Euler model, with kinetic boundary conditions on a solid boundary.

VI. Summary

We have developed and tested different schemes for the direct numerical solution of the Boltzmann transport equation for one-component gas flows at low Knudsen numbers. We have also developed and tested kinetic schemes for continuum gas dynamics based on the Euler system. We determined two strategies of coupling continuum and Boltzmann solvers and explored practical criteria for identifying and separating continuum and kinetic domains. Initial results have been obtained using the new unified continuum/kinetic flow solver (UFS), with both of the two proposed coupling strategies. The work presented in this paper explored the four main ingredients of the UFS: 1) a kinetic solver, 2) a continuum solver, 3) switching criteria, and 4) a coupling mechanism. Future work will focus on improving each of these components and an extension to multicomponent reactive gas mixtures to produce an efficient solver for simulation of industrial problems with different degrees of rarefaction. To our knowledge, this is the first attempt to couple direct Boltzmann and continuum flow solvers to develop a hybrid code with automatic domain decomposition. The work has confirmed that hybrid methods result in significant savings by limiting expensive kinetic solutions only to the regions where they are needed. We have demonstrated that the unified flow solver can automatically introduce or remove kinetic patches to maximize accuracy and efficiency of simulations.

Acknowledgments

This work was supported by U.S. Air Force SBIR Project F33615-03-M-3326. The Technical Monitor of the project was Eswar Josyula.

References

[1]Karniadakis, G. E., and Beskok, A., *Micro Flows: Fundamentals and Simulations,* Springer-Verlag, New York, 2002.

[2]Yen, S. M., "Numerical Solution of the Nonlinear Boltzmann Equation for Nonequilibrium Gas Flow Problems," *Annual Review of Fluid Mechanics*, Vol. 16, 1984, p. 67.

[3]Aristov, V. V., *Direct Methods of Solving the Boltzmann Equation and Study of Nonequilibrium Flows*, Kluwer Academic, Dordrecht, The Netherlands, 2001.

[4]Tan, Z., and Varghese, P., "The $\Delta - \varepsilon$ Method for the Boltzmann Equation," *Journal of Computational Physics*, Vol. 110, No. 2, 1994, pp. 327–340.

[5]Christlib, A. J., Hitchon, W. N. G., Boyd, I. D., and Sun, Q., "Kinetic Description of Flow past a Micro-Pate," *Journal of Computational Physics*, Vol. 195, No. 2, 2004, pp. 508–527.

[6]Ivanov, M. S., and Gimelstein, S. F., "Computational Hypersonic Rarefied Flows," *Annual Review of Fluid Mechanics*, Vol. 30, 1998, p. 469.

[7]Oran, E. S., Oh, C. K., and Cybyk, B. Z., "DSMC: Recent Advances and Applications," *Annual Review of Fluid Mechanics*, Vol. 30, Jan. 1998, pp. 403–441.

[8]Sun, Q., and Boyd, I. D., "A Direct Simulation Method for Subsonic Microscale Gas Flows," *Journal of Computational Physics*, Vol. 179, No. 2, 2002, pp. 400–425.

[9]Wijesinghe, H. S., and Hadjiconstantinou, N. G., "A Discussion of Hybrid Atomistic-Continuum Methods for Multiscale Hydrodynamics," *International Journal for Multiscale Computational Engineering*, Vol. 2, No. 2, 2004, pp. 189–202.

[10]Wu, J.-S., Lian, Y.-Y., Cheng, C., and Koomullil, R., "Development of a Parallel Hybrid Method for the DSMC and NS Solver," 11th National CFD Conf., 2004.

[11]Eggers, J., and Beylich, A. E., "New Algorithms for Application in the Direct Simulation Monte Carlo Method," *Rarefied Gas Dynamics: Theory and Simulations*, edited by B. D. Shizgal and D. P. Weaver, Vol. 159, Progress in Astronautics and Aeronautics, AIAA, Washington, DC, 1994, pp. 166–173.

[12]Eggers, J., and Beylich, A. E., "Development of a Hybrid Scheme and Its Application to a Flat Plate Flow," *Proceedings of the 19th International Symposium on Rarefied Gas Dynamics*, edited by J. Harvey and G. Lord, Vol. 2, Oxford Univ. Press, Oxford, pp. 1216–1222.

[13]Bourgat, J. F., Le Tallec, P., and Tidriri, M. D., "Coupling Boltzmann and Navier–Stokes Equations by Friction," *Journal of Computational Physics*, Vol. 127, 1996, p. 227.

[14]Bourgat, J. F., Le Tallec, P., and Mallinger, F., "Adaptive Coupling Between Boltzmann and Navier–Stokes Equations," *Journal of Computational Physics*, Vol. 136, No. 2, 1997, pp. 51–67.

[15]Wadsworth, D. C., and Erwin, D. A., "Two-Dimensional Hybrid Continuum/Particle Approach for Rarefied Flows," AIAA Paper 92-2975, 1992.

[16]Hash, D. B., and Hassan, H. A., "Two-Dimensional Coupling Issues of Hybrid DSMC/Navier–Stokes Solvers," AIAA Paper 97-2507, 1997.

[17]Garsia, A. L., Bell, J. B., Crutchfield, W. Y., and Alder, B. J., "Adaptive Mesh and Algorithm Refinement Using Direct Simulation Monte Carlo," *Journal of Computational Physics*, Vol. 154, No. 1, 1999, pp. 134–155.

[18]Wijesinghe, H. S., Hornung, R. D., Garsia, A. L., and Hadjiconstantinou, N. G., "Three-Dimensional Hybrid Continuum-Atomistic Simulations for Multiscale Hydrodynamics," *Journal of Fluids Engineering*, Vol. 126, No. 5, 2004, pp. 768–777.

[19]Crouseilles, N., Degond, P., and Lemou, M., "A Hybrid Kinetic/Fluid Models for Solving the Gas Dynamics Boltzmann-BGK Equation," *Journal of Computational Physics*, Vol. 199, No. 2, 2004, pp. 776–808.

[20]Beylich, A. E., "Solving the Kinetic Equation for All Knudsen Numbers," *Physics of Fluids*, Vol. 12, No. 2, 2000, pp. 444–465.

[21]Beylich, A. E., "Kinetics of Thermalization in Shock Waves," *Physics of Fluids*, Vol. 14, No. 8, 2002, pp. 2683–2699.

[22]Tiwari, S., and Klar, A., "An Adaptive Domain Decomposition Procedure for Boltzmann and Euler Equations," *Journal of Computational and Applied Mathematics*, Vol. 90, 1998, pp. 223–237.

[23]Le Tallec, P., and Mallinger, F., "Coupling Boltzmann and Navier–Stokes Equations by Half Fluxes," *Journal of Computational Physics*, Vol. 136, No. 1, 1997, pp. 51–67.

[24]Tiwari, S., "Coupling of the Boltzmann and Euler Equations with Authomatic Domain Decomposition," *Journal of Computational Physics*, Vol. 144, 1998, p. 710.

[25]Popov, S. P., and Tcheremissine, F. G., *Rarefied Gas Dynamics, 24th International Symposium, AIP Conference Proceedings*, American Inst. of Physics (to be published).

[26]Carlson, H. A., Roveda, R., Boyd, I. D., and Candler, G. V., "A Hybrid CFD-DSMC Method of Modeling Continuum-Rarefied Flows," AIAA Paper 2004-1180, Jan. 2004.

[27]Cercignani, C., *The Boltzmann Equation and its Applications*, Springer-Verlag, New York, 1988.

[28]Sone, Y., *Kinetic Theory and Fluid Dynamics*, Birkhauser, Boston, 2002.

[29]Aristov, V. V., and Tcheremissine, F. G., "Conservative Splitting Method for Solving the Boltzmann Equation," *USSR Journal of Computational Mathematics and Mathematical Physics*, Vol. 20, No. 1, 1980, p. 208.

[30]Tcheremissine, F. G., "Conservative Evaluation of Boltzmann Collisional Integral in Discrete Ordinates Approximation," *Computers Math. App.*, Vol. 35, No. 1/2, 1998, p. 215.

[31]Frolova, A. A., "Computation of a Flow Around Cylindrical Bodies at Small Knudsen Numbers," *Computational Rarefied Gas Dynamics*, Computing Center of Russian Academy of Sciences, Moscow, 2000, p. 27.

[32]Pullin, D. I., "Direct Simulation Methods for Compressible Inviscid Ideal Gas Flow," *Journal of Computational Physics*, Vol. 34, No. 2, 1980, pp. 231–244.

[33]Reitz, R. D., "One Dimensional Compressible Gasdynamics Calculations Using the Boltzmann Equations," *Journal of Computational Physics*, Vol. 42, No. 1, 1981, pp. 108–123.

[34]Aristov, V. V., and Tcheremissine, F. G., "Solving the Euler and Navier–Stokes Equations on the Basis of the Operator Splitting of the Kinetic Equations," *Doklady of USSR Academy of Sciences*, Vol. 272, No. 3, 1983, p. 555.

[35]Aristov, V. V., and Tcheremissine, F. G., "The Kinetic Numerical Method for Rarefied and Continuum Gas Flows," *Rarefied Gas Dynamics*, edited by O. M. Belotserkovskii, M. N. Kogan, S. S. Kutateladse, and A. K. Rebrov, Plenum, New York, 1985, p. 269.

[36]Potkin, V. V., "A Kinetic Scheme for Gas-Dynamic Equations in Lagrange Coordinates," *USSR Journal of Computational Mathematics and Mathematical Physics*, Vol. 15, No. 6, 1975, p. 227.

[37]Mandal, J. C., and Deshpande, S. M., "Kinetic Flux Vector Splitting for Euler Equations," *Computers and Fluids*, Vol. 23, 1994, p. 447.

[38]Chou, S. Y., and Baganoff, D., "Kinetic Flux-Vector Splitting for the Navier–Stokes Equations," *Journal of Computational Physics*, Vol. 130, No. 2, 1997, pp. 217–230.

[39]Xu, K., "A Gas-Kinetic BGK Scheme for the Navier–Stokes Equations and Its Connection with Artificial Dissipation and Godunov Method," *Journal of Computational Physics*, Vol. 171, No. 1, 2001, pp. 289–335.

[40]Ohwada, T., "On the Construction of Kinetic Schemes," *Journal of Computational Physics*, Vol. 177, No. 1, 2002, pp. 156–175.

[41]Ohwada, T., and Kobayashi, S., "Management of Discontinuous Reconstruction in Kinetic Schemes," *Journal of Computational Physics*, Vol. 197, No. 1, 2004, pp. 116–138.

[42]Ohshawa, T., and Ohwada, T., "Deterministic Hybrid Computations of Rarefied Gas Flows," *Rarefied Gas Dynamics, 23rd International Symposium*, edited by A. D. Ketsdever and E. P. Muntz, AIP Conference Proceedings, Vol. 663, American Inst. of Physics, New York, 2003, p. 931.

[43]Xu, K., "A Gas-Kinetic BGK Scheme for Compressible Navier–Stokes Equation," ICASE Rept. 2000-38, 2000.

[44]Woodward, P., and Colella, P., "The Numerical Simulations of Two Dimensional Fluid Flow with Strong Shocks," *Journal of Computational Physics*, Vol. 54, No. 1, 1984, pp. 115–173.

[45]Bird, G. A., "Breakdown of Translational and Rotational Equilibrium in Gaseous Expansions," *AIAA Journal*, Vol. 8, 1970, p. 1998.

[46]Wang, W.-L., and Boyd, I. D., "Predicting Continuum Breakdown in Hypersonic Viscous Flows," *Physics of Fluids*, Vol. 15, No. 1, 2003, pp. 91–100.

[47]Boyd, I. D., Chen, G., and Candler, G.V., "Predicting Failure of the Continuum Fluid Equations in Translational Hypersonic Flows," *Physics of Fluids*, Vol. 7, No. 1, 1995, pp. 210–219.

I. Boyd
Associate Editor